Est. 1984

ORIENTAL JOURNAL OF CHEMISTRY
An International Open Free Access, Peer Reviewed Research Journal

www.orientjchem.org

ISSN: 0970-020 X
CODEN: OJCHEG
2018, Vol. 34, No.(1):
Pg. 362-370

Catalytic Conversion of CO_2/H_2 into Alcohol Using Modified Lampung–Zeolite as Catalyst

RUDY SITUMEANG

Department of Chemistry, University of Lampung, Indonesia, Jln. Prof. Soemantri, Brodjonegoro, No 1 Bandar Lampung 35145, Indonesia.
Corresponding author E-mail: rudy.tahan@fmipa.unila.ac.id

http://dx.doi.org/10.13005/ojc/340139

(Received: September 22, 2017; Accepted: December 05, 2017)

ABSTRACT

This work was carried out to study the potency of modified lampung-zeolite as catalyst for conversion of CO_2/H_2 into alcohol compounds. The zeolite was activated using 0.1N nitric acid, by soaking the zeolite in the acid for 2 h and then impregnated by Fe_2O_3 with varied content of 1 – 7% (g/g). To examine its activity, the catalyst was used in CO_2/H_2 conversion experiment at different temperatures (200 to 400 ^oC). The experimental results indicated the zeolite impregnated by iron ions exhibits catalytic activity, and the highest alcohol formation (26000 ppm) was achieved by 5% Fe_2O_3 doped zeolite at 200 ^oC. X-ray diffraction of washed-zeolite revealed that its crystalline phase is a clinoptilolite type of zeolite with monoclinic structure. Infra-red spectra analysis proved that 5% Fe_2O_3 doped zeolite has Bronsted-Lowry and Lewis acid sites presenting at wave number of 1466 and 1648 cm^{-1} respectively. Furthermore, SEM analysis implied that Lampung zeolite has a channel pattern and relatively good porous distribution.

Keywords: Zeolite, CO_2 , Hydrogenation, Acid sites, Alcohols.

INTRODUCTION

In respond to fossil fuels depletion and concern on environmental impacts, primarily due to CO_2 produced from their utilization, conversion of CO_2 into various chemicals useful as alternative and renewable fuel has been intensively investigated in the last few decades. For this purpose, different catalysts have been tested and in general, the results obtained indicate that catalysts play very important roles in governing the yield and type of product resulted. As an example, $Cu_{20}Mo_2C$/M41 catalyst abled to produce 5.5% yield of methanol at a CO_2 conversion of 8.8%[1]. Other groups of research using different kinds of catalysts such as Fe-Zn-Zr/HY composite catalyst abled to obtain isoalkanes at 340^oC as much as 20% CO_2 conversion, 45% selectivity to i-C_4, and

9% yield[2]; CuO-ZnO-TiO_2 catalyst operated at 493 K gave 35% conversion of CO_2 with the selectivity of 52.3% to ethanol[3]; K/Cu-Zn-Fe catalyst abled to produced ethanol at 300 °C as much as 90% CO_2 conversion and 85 % selectivity to ethanol[4]; Co-Fe bimetallic catalyst operated at 200 – 270 °C obtained 27% of CO_2 conversion and 71% of CH_4 selectivity [5].

Another type of materials that exhibit catalytic activity is natural zeolite, that can be found in many different places around the world. In Indonesia, one of the regions that has natural zeolite deposit is Lampung Province. Due to their availability and chemical as well as physical characteristics, natural zeolites have been used as catalyst for different reactions, for examples, pure phase β-zeolite operated at 120 °C and atmospheric pressure abled to obtain 90% yield of ethyl acetate from 80% acetic acid conversion[6]; Pacitan-Natural zeolite as catalyst support for transesterification of palm oil abled to produce 96% yield of both methyl palmitate and stearate at 60 °C[7]; and H-Mordenite type of zeolite operated at 423K abled to produce 12% glucose from 0.05 g Cellulose in 5 mL water[8].

To improve their catalytic performance, natural zeolites are commonly activated or modified by addition of other active sites. Several studies revealed that addition of active sites significantly increased catalytic activity of natural zeolites. For examples, clinoptilolite type of natural zeolite impregnated by KOH and operated at 350 – 440 °C and abled to gain 90% yield of liquid fuel from natural triacylglicerol[9]; modified natural zeolite from Kidul mountain of java island abled to convert ethanol as much as 15% and produced 3% yield of diethyl ether at 140 °C[10]; and modified natural clinoptilolite from Bayah – Indonesia operated at 60 – 80 °C and abled to obtain almost 100% glycerol carbonate from 25% conversion of glycerol[11]. In hydrogenation of CO_2 reaction, modified natural zeolite with 5% nickel abled to produce methane with the 96% selectivity and 10% conversion of CO_2 at 300 °C reaction temperature[12].

In recognizing the important role of additional active sites on performance of natural zeolites, in this study, Lampung zeolite was modified by addition of different amounts of iron oxides as active sites. The modified zeolites were subsequently calcined at 600 °C and then tested as catalyst for conversion of CO_2 into alcohol at a temperature range of 200 – 400 °C.

MATERIAL AND METHODS

The chemical used in this study, natural zeolite, nitric acid, Fe-nitrates, and NH_3 are reagents grade obtained from Merck & Co. The main equipments used in this study are Fourier Transform Infrared (FTIR) spectrophotometer (Shimadzu Prestige-21), Scanning Electron Microscope (SEM, Philips-XL), Philips X-ray diffractometer (XRD) model PW 1710 with Cu-Kα radiation, and Gas Chromatography (Agilent 7890B) with Flame Ionization detector .

Modification of natural zeolite

Modification of natural zeolite was carried out in two steps. The first treatment was carried out by soaking the sample in 0.1N nitric acid solution for 2 h with continuous shaking. The mixture was filtered and the solid was repeatedly rinsed with distilled water to remove the excess of acid. At the second step, the solid was calcined at 600 °C for 2 h (increased by 2 °C min^{-1}), and then impregnated with 1 – 7% Fe_2O_3 by soaking zeolite in Fe-nitrates solution and heated at 80 °C until water solvent evaporated. Finally, the samples were recalcined at 600 °C for 2 hours.

Characterizations

XRD Analysis

The XRD powder patterns were obtained in a Philips diffractometer Model PW 1710, using Cu K_a radiation and operating at 40 kV and 40 mA. The scanning range of 2θ angle was set from 5 to 70°, with a step size of 0.02°/ s. The crystalline phases identification of the samples was analysed and calculated by using search and match program (Version 2.1) and Rietveld Method, respectively[13].

FTIR Analysis

Sample was treated in vaccumized dessicator after heating at 120 °C and then, the vapour of liquid pyridine was allowed to contact the sample located inside of vaccum dessicator for 24 hours. After taking out from dessicator and allowing on air for 2 h, a small amount of sample was finally mixed to KBr powder (sample/KBr ratio

less than 1%) to form a pellet at ambient temperature and was ready to be analysed by putting it on quartz cell of FTIR (Shimadzu) in the wave number range of 400 – 4000 cm^{-1}. This procedure had already been used in the previous work[14, 15].

SEM analysis

A small quantity of the sample was mounted on a stub with an adhesive coated by 40 – 60 nm of gold or other conducting materials. Then, the crystal morphology and size of the samples were observed[16, 17].

RESULTS AND DISCUSSION

Structural analysis

Materials that have been prepared were characterized using some instruments such as X – ray diffraction, (FTIR) spectroscopy, and SEM as explained as follow.

X-Ray Diffraction Analysis

Qualitative XRD analysis was conducted by comparing the diffraction lines of zeolite sample with those in standard from the ICCD files and showed that the major phase obtained for the sample is clinoptilolite phase. The minor phases was also obtained such as Quartz and cristobalite as shown in Fig. 1 below. This washed zeolite, however, cliptonilolite is accordance with JCPD File # 39-1383[18], which has a monoclinic structure.

Furthermore, to obtain quantitative information from the zeolite, Rietveld analysis is used to obtain unit cell parameters and distinguish the phase composition clearly. As shown in Fig. 2, one of the XRD Rietveld analysis has been plotted for the zeolite. This result was satisfied by examining the goodness of fitting value ($\chi^2 \leq 4$).

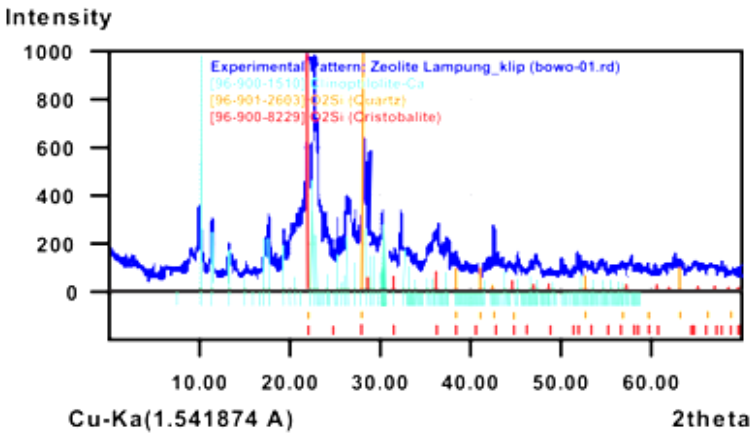

Fig. 1.Diffractogram of natural zeolite after washing with 0.1N nitric acid in 2 h and then calcining at 600 °C measurements.

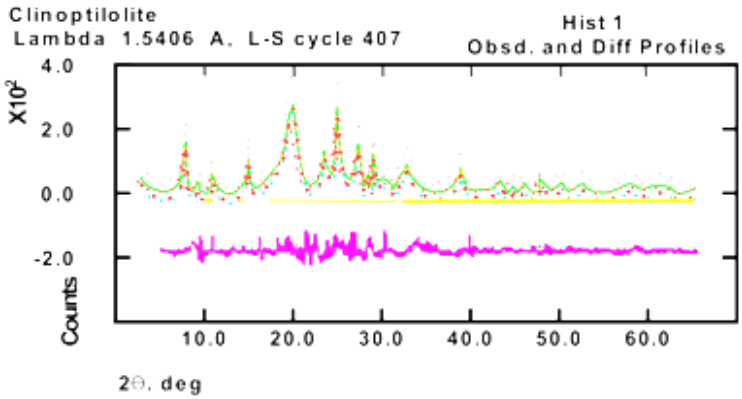

Fig. 2. XRD Rietveld Plot for zeolite sample after washing and calcining at 600 °C. The Observed data are shown by the (+) red sign, and the calculated data by a solid line (Green). The vertical lines (Yellow, Green and purple, indicates hkl indices of three phases), The purple line below the vertical lines is the difference profile.

In addition, this fitting plot indicates the accomplishment of the Rietveld refinement, in which the different plot between calculated and observed patterns shows relatively minor fluctuation. This result also proved that the output of the refinement can be used to provide further information such as phase composition, unit cell parameters, and atomic position in space.

Table. 1 shows phase composition, unit cell parameters, crystal system, and weight percentage from Rietveld refinement with XRD data for zeolite sample washed and calcined at 600 °C for 2 hours. Evidently, the weight percentage for clinoptilolite, quartz, and crystoballite phases is 65.9, 31.6, 2.5, respectively. The relatively high quantity of quartz is probably affected by both acid washing and calcining at 600 °C since natural zeolite dehydrated when it had been heated above 500 °C[13,19]. Then,structrural phases, the samples, with different iron oxides content were characterized and the X-ray diffraction patterns of the samples were compiled in Fig. 3. As can be shown in Fig. 3, the diffractogram are generally similar, with only some differences in the intensity of certain position of the representative peaks of zeolite (clinoptilolite form). For instanse, at 2θ of 32.93° as a major peak of Fe_2O_3 (PDF-330664) is more pronounced as quantity of Fe_2O_3 - dopant increased, as particular for 7% Fe_2O_3 dopant. In a ragion of 20° through 33°, as shown in Fig.3, represent clinoptilolite type and then the representative peaks (i.e intensity and 2θ) changed slightly as dopant content augmounted. The effect of dopant addition into zeolite parameter cells is investigated by Rietveld calculation.

Table. 1: Rietveld Refinement results of Lampung Zeolite (R_{wp} = 21.51; R_p = 16.97 ; χ^2 = 1.317)

No.	Phase Identification	Unit Cell Parameters a (Å)	b (Å)	c (Å)	V (Å³)	α	β	λ	Crystal System	Weight Percentage (% wt)
1.	Clinoptilolite	19.586	19.177	7.888	2661.6	90°	116.7°	90°	Monoclinic	65.9
2.	Quartz	4.985	4.985	5.287	113.7	90°	90°	120°	Hexagonal	31.6
3.	Cristobalite	17.632	17.941	7.400	2097.0	90°	90°	90°	Tetragonal	2.5

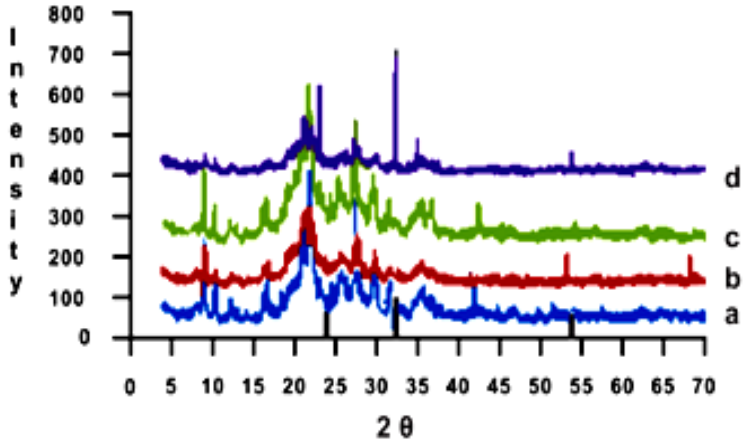

Fig. 3. Diffractograms of Fe_2O_3 doped zeolite with variation of dopant : (a). 1% Fe_2O_3, (b). 3% Fe_2O_3, (c). 5% Fe_2O_3, and (d). 7% Fe_2O_3 and a reference of Fe_2O_3 phase (black – bar ; PDF330664). To evaluate the effect of the iron oxides quantities on the stability ofLampung – zeolite.

Quantitative analysis of modified zeolite using Rietveld method is presented in Table. 2 below, and analysis of Rietveld calculation has shown a very good result since its Goodness of Fitting value (χ^2 or GOF) had been obtained satisfying the required values of ≤4. The effect of Fe_2O_3 addition into zeolite, proved that structure of zeolite is not sufficiently influenced by the formation of hematite – Fe_2O_3 crystalline phase. In the other word, the formation of hematite-Fe_2O_3 is not happened exactly inside the channels of zeolite since the crystalline structure of a washed natural zeolite has still existed. This evident is also found by Cheng *et al.,* while loading of Fe and Ni into HZSM – 5 catalyst [20].

Table. 2: Rietveld refinement results of Zeolite doped

No.	Zeolite added with	Unit cell Parameters a(Å)	b(Å)	c(Å)	χ^2 (GOF)*	Crystalline Phase(s) dominant
1	0 % Fe_2O_3	19.586	19.197	7.888	1.317	clinoptilolite
2	1 % Fe_2O_3	19.588	19.196	7.898	1.429	clinoptilolite
3	3 % Fe_2O_3	19.587	19.198	7.888	1.547	clinoptilolite
4	5 % Fe_2O_3	19.589	19.197	7.889	1.671	clinoptilolite
5	7 % Fe_2O_3	19.587	19.199	7.886	1.537	Clinoptilolite & Hematite

Microstructure Analysis

The surface characteristic is very important to the catalytic application involving the surface interaction (adorption – desorption) process. For this reason, the samples investigated in this study were characterized using SEM technique[17]. The SEM micrographs of some samples are shown in Fig. 4. As can be seen in Fig. 4, The SEM micrographs of washed-zeolite and some Fe_2O_3 doped zeolite samples display clearly a porous structure. The topography of these samples told that its texture is relatively homogeneous and amorphous. Also, its morphology suggesting there is the effect of Fe_2O_3 dopant on its shape and channel. However, by careful inspection of certain region, the varied diameter size of channel and some ductiles spots are observed. Furthermore, some ductiles has a diameter of 0.1 – 3 mm (red-arrow) and others have diameter even higher than 3 mm. Also there are some brittle channel parts (green-arrow) . This brittle channel part is happened probably because of washing, dopant-adding and calcining process. In general the Fe_2O_3 addition into zeolite did not damage the channel structure of zeolite as can be seen.

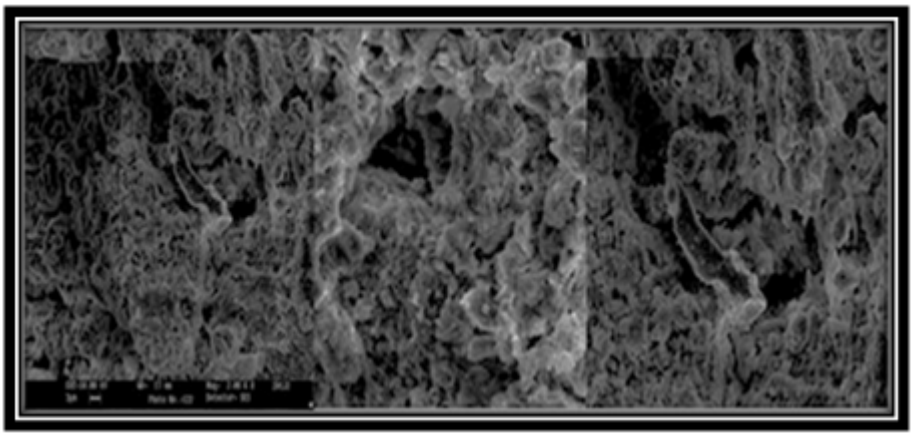

Fig. 4. Micrographs of washed zeolite (a) 3% Fe_2O_3 doped zeolite (b) and 5% Fe_2O_3 dopedZeolite (c) after calcining at 600 °C for 2 h (Mag. = 2.00k x), from left to right.

Acidity Analysis

To identify the functional group present in the sample which is primarily to know the existence of Lewis and BrØnsted-Lowry acid sites, the Fourier transform infra-red spectroscopy is applied in this study. These characteristics are very important to determine the performance of catalyst. The FTIR spectrum of washed – zeolite as an example is shown in Figure. 5.

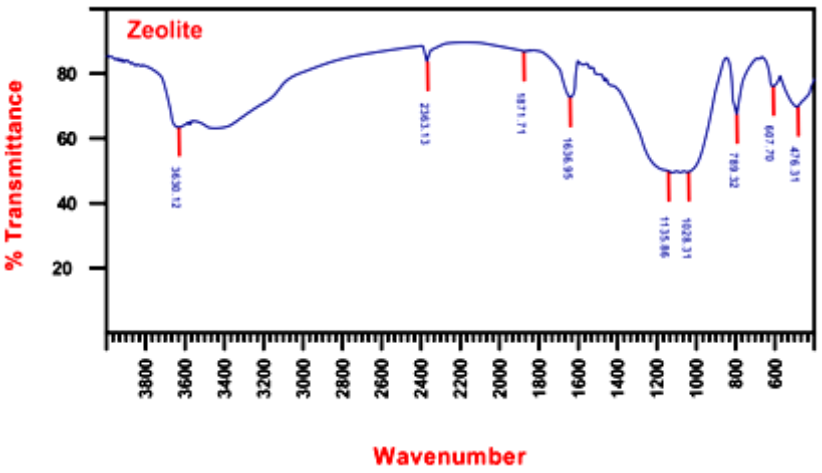

Fig. 5. Infra red spectra of washed zeolite after treating with Ammonia

As can be seen in Fig. 5 above, the absorption bands representing both acid sites were proved by the existing of Zeolite $–NH_3$ (as Lewis acid site) and/or zeolite $–NH_4^+$(as Bronsted – Lowry acid site) vibrations. In general, wavenumber region of 3100 – 3700 cm^{-1} refers to stretching vibrations and wavenumber below 2500 cm^{-1} relates to bending and rocking vibrations. In Fig. 5, Lewis acid sites appeared to wave number of 1636.95 cm^{-1} and little peaks in region of 1450 – 1550 cm^{-1}. However, Bronsted – Lowry acid sites appeared at wavenumber of 1400 – 1440 cm^{-1}. Furthermore region below 1200 cm^{-1} belongs to fingerprint pattern of zeolite. Strong stretching vibrations of the bond Si – O – Si, Al – O – Si, and Al – O – Si appeared at the wavenumber range of 1000 – 1136 cm^{-1} and 789 cm^{-1}. These peaks indicate that tetrahedral linkage arrangement in tetrahedron $(Al,Si)O_4$ still remain after washing and calcining at 600 °C. The peaks that were appeared at 476 and 608 cm^{-1} show the bending vibrations of tetrahedral linkage.

In the Fe_2O_3 doped zeolites samples investigated, as can be seen in Fig. 6, the spectra are pratically similar in terms of the absorption bands for acid sites characteristics, with only some minor differences in intensities and wave numbers,

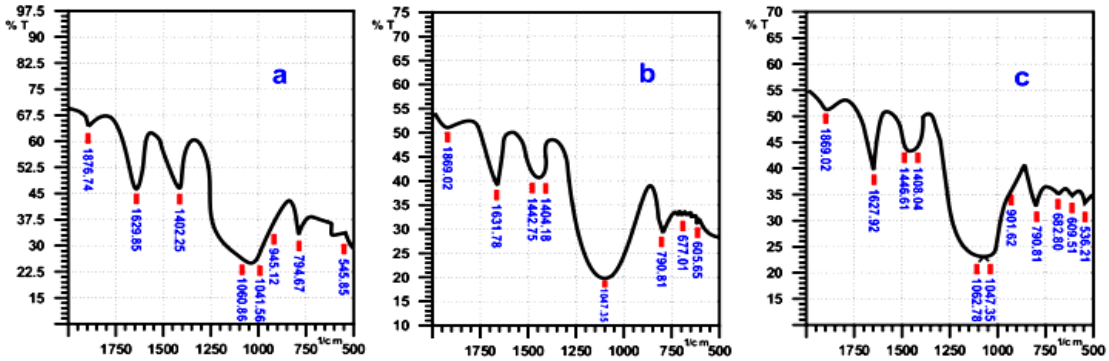

Fig. 6. FTIR spectra of some zeolites doped with : (a) 1% Fe_2O_3, (b) 3% Fe_2O_3, and (c) 5% Fe_2O_3 after treating with ammonia

depending on the quantity of Fe_2O_3 doped into zeolite. The existence of Lewis acid sites is indicated by the vibration bands resulted from stretching vibration, located at 1628 cm^{-1} for 1% Fe_2O_3 doped zeolite; 1650 and 1632 cm^{-1} for 3% Fe_2O_3 doped zeolite, and then 1648 and 1628 cm^{-1} for 5% Fe_2O_3 doped zeolite. While the existence of Bronsted-Lowry acid sites is shown by the vibration bands resulted from stretching vibration, located at 1466 and 1400 cm^{-1} for 1% Fe_2O_3 doped zeolite; 1443 and 1404 cm^{-1} for 3% Fe_2O_3 doped zeolite, and then 1466 and 1408 cm^{-1} for 5% Fe_2O_3 doped zeolite. By comparing the intensities of the absorption bands corresponding to Lewis and Bronsted-Lowry acid sites, it can be concluded that acid property of the Fe_2O_3 doped zeolite samples is dominated by the Lewis acid sites, and there is a tendency that the Lewis acid strength relatively increases with increased Fe content in the samples. The increase of acid properties is also found while Fe and Co was loaded in SiO_2[21]. In finger print region of spectra, the absorption band representing stretching and bending vibrations of Fe-O were detected at 613, 677, and 663 cm^{-1} for 1%, 3%, and 5% Fe_2O_3 doped, respectively[22, 23].

Catalytic Activity

Hydrogenation of carbon dioxide was run in the reactor (U-type) with the variation of temperature, 200-400 °C and the gas flow of 3 L/h consisting CO_2/H_2 ratio of 0.25. The results are displayed in Fig. 7 and Figure. 8 below.

As can be seen in Fig. 7, zeolite washed is active to convert CO_2 into alcohol eventhough its activity was low, 1000 ppm of methanol at 200 °C was obtained. It can be explained that CO_2 and H_2 molecules was attached strong enough to form C_1 ionic molecule on the surfaces of catalyst before forming CH_3OH molecules. In higher temperature, 300 and 400 °C, its activity became very low. It can be implied that as temperature increase the contact time between CO_2 and H_2 molecules into zeolite surfaces shorter so that there are no sufficient interaction to produce more methanol. Other alcohols such as ethanol, propanol, and butanol were also formed but its amount was too small compared to methanol formation at 200 °C. Besides insufficient interaction, it can also be explained that the most methanol formed was oxidized in advance as temperature increased.

The effect of Fe_2O_3 dopant in zeolite activity to convert CO_2 into alcohol is shown in Fig. 8. In general, the activity of zeolite is abruptly increased by adding Fe_2O_3. Eventhough, Fe_2O_3 itself that has been prepared with the same method did not show an activity. In addition, by looking at certain temperature, for instance 200 °C, the alcohol result is quite well distributed using 5% Fe_2O_3 doped Zeolite. The well distribution of alcohol results (i.e. CH_3OH, C_2H_5OH, C_3H_7OH, and C_4H_9OH) using 5% Fe_2O_3 doped zeolite can be explained that both CO_2 and H_2 molecules adsorbed on the surface of this catalyst have enough time to form C^+, C_2^+, C_3^+ and C_4^+ species, so higher alcohol can be obtained as illustrated on Scheme 1 below[24, 25]. Another reason why a longer chain of alcohol was formed greater than that of methanol is the Lewis acid sites of zeolite located at relatively high wavenumber, about 1640 cm^{-1}, plays an important role in binding CO_2 and H_2 molecules on the surface. Therefore, further oxidation is happened.

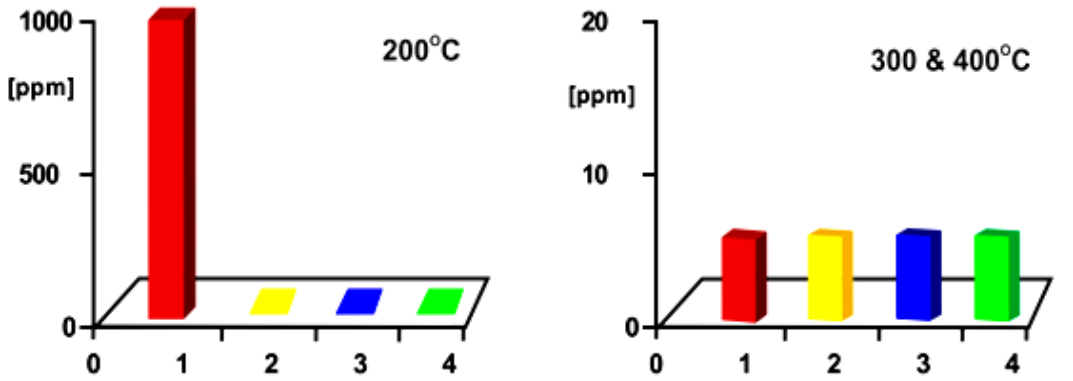

Fig. 7. Alcohol results from CO_2/H_2 reaction using zeolite washed as catalyst. Index 1, 2, 3, and 4 refers to methanol, ethanol, propanol and butanol, respectively and standard deviation 2.4%

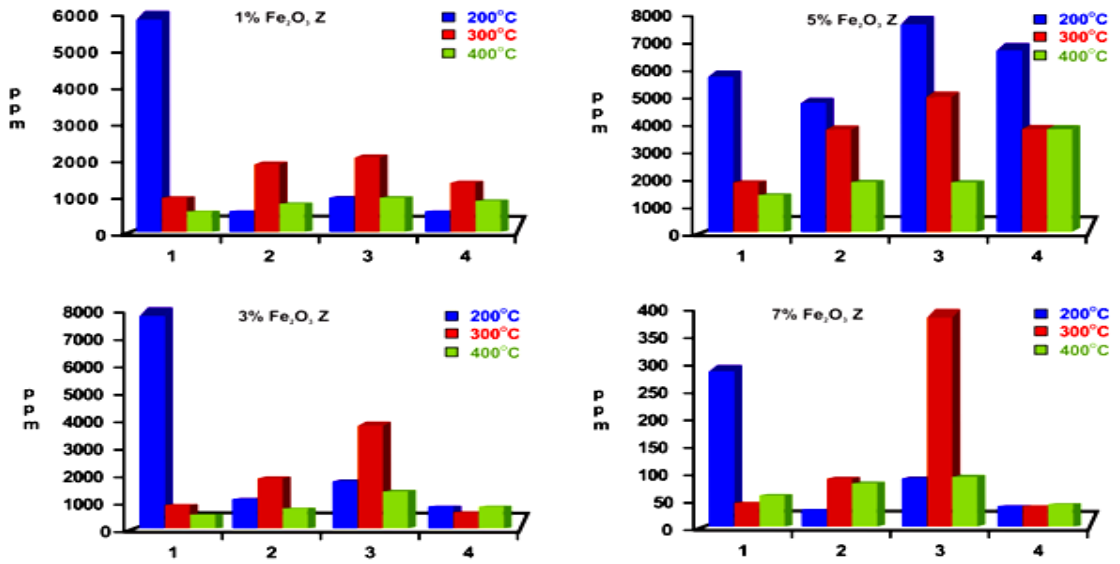

Fig. 8.Alcohol results from CO_2/H_2 reaction using varied Fe_2O_3 doped zeolite as catalyst. Index 1, 2, 3, and 4 refers to methanol, ethanol, propanol and butanol, respectively and standard deviation 2.4%.

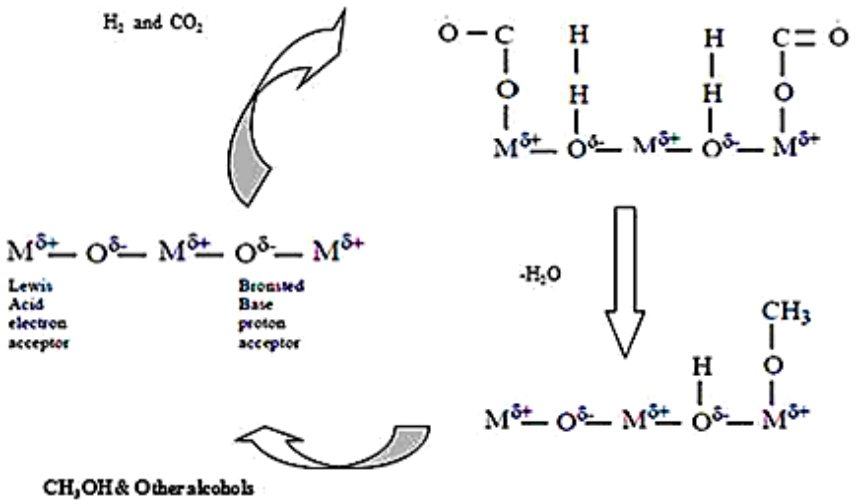

Scheme 1: Illustration of alcohols formation in CO_2/H_2 reaction on Lampung Zeolite Catalyst

CONCLUSION

It can be concluded that modified zeolite of Lampung is active as a catalyst for converting CO_2 and H_2 into alcohol in the temperature range of 200 – 400 °C. By adding and varying Fe_2O_3 content into zeolite, its activity is ameliorated and the higher alcohol result is formed. Regarding on its acid behaviour, it can be implied that the activity of modified Lampung-zeolite becomes better as acid characteristic more pronounced.

ACKNOWLEDGEMENT

The author wish to thank and appreciate the Directorate General Higher Education Republic of Indonesia for research fund provided through Competitive Research Grant program with a contract no. 267/H26/PL/2016.

REFERENCES

1. Liu, X.; Song, Y.; Geng, W.; Li, H.; Xiao, L.; Wu, W.*Catal.,* **2016**, *6*, 75 – 87.
2. Ni, X.;Tan, Y.;Han, Y.; Tsubaki, N. *Catal. Commun.,* **2007**, *8*, 1711 – 1714.
3. Xiao, J.; Mao, D.; Guo, X.; Yu, J. *Energy Technol.,* **2015**, *3*, 32 – 39.
4. Li, S.;Guo, H.;Luo, C.; Zhang, H.;Xiong, L.;Chen, X.; Ma, L.*Catal. Lett.,* **2013**, *143*, 345 – 355.
5. Muthu, K.; Gnanamani, G.J.; Hamdeh ,H.H.; Shafer, W.D.; Liu, F.; Hopps, S.D.; Thomas, G.A.; Davis, B.H.*ACS Catal.*, **2016**, *6*, 913 – 927.
6. Yue, Y.;Liu, H.;Zhou, Y.;Bai, Z.; Bao, X. *Appl. Clay Scie.,* **2016**, *126*, 1 – 6.
7. Kusuma, R.I.; Hadinoto, J.P.; Ayucitra, A.; Soetaredjo, F.E.; Ismadji, S.*Appl. Clay Scie.*, **2013**, *74*, 121 – 126.
8. De Vyvwe, S.V.; Peng, L.; Geboers, J.; Schepers, H.; de Clippel, F.; Gommes, C.J.; Goderis, B.; Jacobs, P.A.; Sels B.F. *Green Chem.,* **2010**, *12*, 1560.
9. Cvengroš, J.; Buzetzki, E.;Švaòová, K. *44th Intern. Petrol. Conf. Bratislava, Slovak Republic, September 21 – 22nd,* 1 - 8., **2012**.
10. Widayat, W.; Roesyadi, A.; Rachimoellah, M. *Internat. J. Sci. Eng.,* **2013**, *4*, 6 – 10.
11. Mahdi, H.I.; Irawan, E.; Nuryoto, N.; Jayanudin, J.; Sulistyo, H.; Sediawan, W.B.; Muraza, O. *Waste and Biomass Valor.,* **2016**, *7*, 1349 - 1356.
12. Bacariza, M.C.; Garcia, I.; Westermann, A.; Ribeiro, M.F.; Lopes, J.M.; Henriques, C. *Topics in Catal.,* **2016**, *59*, 314 – 325.
13. Hutching, G.J.; Comninos, H.; Copperth waite, R.G.; van Rensburg, R.; Hugo, M. *J. Appl.Crystallogr.,* **1969**, *2*, 65 – 71.
14. Parry E.P., *J. Catal.,* **1963**, *2*, 371 – 379.
15. Situmeang, R.; Manurung, P.; Sulistiyo, S.T.; Hadi, S.; Simanjuntak, W.; Sembiring, S. *Asian J. Chem.,* **2015**, *27*, 1138 – 1142.
16. Drbohlavova, J.; Adam, V.; Kizek, R.; Hubalek, J.; *Int. J. Mol. Sci.,* **2009,** *10*, 656 – 673.
17. Hanke L.D., Handbook of Analytical Methods for Materials. Materials Evaluation and Engineering Inc. Plymouth, USA., **2001**,35 – 38.
18. Gottardi G., Galli E., Natural Zeolite: Pottasium Sodium Calcium Alumminum Silicate hydrate (Clinoptilolite), Springer–Velag, Tokyo., **1985**, 341.
19. Breger, I.A.; Chandler, J.C.; Zubovic, P. *The Am. Miner.,* **1970**, *55*, 826 – 840.
20. Cheng, S.; Wei, L.; Julson, J.; Muthukumarappan, K.; Kharel, P.R. *Fuel Proc. Tehcn.,* **2017**, *167*, 117 – 126
21. Cheng, S.; Wei, L.; Julson, J.; Rabnawaz, M. *Energ. Conv. Manag.,* **2017**, *150*, 331 – 342.
22. Zhiqiang, W.; Hongxia, Q.; Hua, Y.; Cairong, Z.; Xiaoyan, Y. *J. Alloys. Compd.,* **2009**, *479*, 855 – 858.
23. Kim, J.S.; Ahn, J.R.; Lee, C.W.; Murakami, Y.; Shindo, D. *J. Mater. Chem.,* **2001**, *11*, 3373 – 3376.
24. Kienneman, A.; Boujana, S.V.S.; Diagne, C.; Chaumette, P. *Stud. Surf. Sci. Catal.,* **1993**, *75*, 1479.
25. Jung, K.T.; Bell, A.T. *J. Catal.,* **2001**, *204*, 339 - 347.